Available online at www.sciencedirect.com

SciVerse ScienceDirect

journal homepage: www.elsevier.com/locate/ijrefrig

Experimental and numerical investigation of the influence of the two-phase ejector geometry on the performance of the R744 heat pump

Krzysztof Banasiak [a,*], *Armin Hafner* [b], *Trond Andresen* [b]

[a] *Institute of Thermal Technology, Silesian University of Technology, Konarskiego 22, Gliwice 44-100, Poland*
[b] *SINTEF Energi, Kolbjørn Hejes v. 1D, Trondheim 7465, Norway*

ARTICLE INFO

Article history:
Received 9 January 2012
Received in revised form
13 April 2012
Accepted 13 April 2012
Available online 21 April 2012

Keywords:
R744 heat pump
Expansion work recovery
Two-phase ejector
Geometry optimisation

ABSTRACT

An experimental and numerical investigation of the optimum ejector geometry for a small-capacity R744 heat pump was performed. Different ejector configurations were examined, including various lengths and diameters of the mixer and various angles of divergence for the diffuser. Based on a simplified, one-dimensional ejector model, an optimisation of the ejector geometry was performed. Based on both the numerical simulation and experimental work, the ejector efficiency proved to be notably dependent on the mixer length and the diameter, as well as on the diffuser divergence angle. The maximum increase in the coefficient of performance (COP) was 8% over a system with a conventional expansion valve.

Etude expérimentale et numérique sur l'influence de la géométrie de l'éjecteur diphasique sur la performance d'une pompe à chaleur au R744

Mots clés : Pompe à chaleur ; Dioxyde de carbone ; R744 ; Récupération du travail de détente ; éjecteur diphasique ; Géométrie ; Optimisation

* *Corresponding author*. Tel.: +48 32 237 10 19; fax: +48 32 237 28 72.
E-mail address: krzysztof.banasiak@polsl.pl (K. Banasiak).
0140-7007/$ – see front matter © 2012 Elsevier Ltd and IIR. All rights reserved.
doi:10.1016/j.ijrefrig.2012.04.012

Nomenclature

D	channel diameter, m
h	specific enthalpy, J kg^{-1}
L	length, m
$\dot{m}$	mass flow rate, kg s^{-1}
p	pressure, Pa
s	specific entropy, J kg^{-1} K^{-1}
T	temperature, K
u	uncertainty of a measured variable

Greek symbols

α	angle of divergence (full cone), °

Subscripts

DIF	diffuser
MIX	mixer
MN	motive nozzle
out	outlet
SN	suction nozzle

1. Introduction

The use of ejectors in R744 refrigeration systems is one of the most promising methods to increase the system efficiency and reduce the throttling loss, as discussed in Elbel and Hrnjak (2008) and Elbel (2011). In addition, the ejector's simplicity (i.e., it has no moving parts) compared to expanders, its low cost and its reasonable efficiency make it very attractive. However, ejector-equipped R744 transcritical cycle installations, where the working fluid passes from the supercritical phase across the saturated state into the two-phase condition, present complicated issues for both analytical and experimental investigations, especially those aimed at optimisation of the ejector geometry.

Cizungu et al. (2005) performed a pseudo-one-dimensional (1D) design and an off-design numerical analysis for ammonia and ammonia-water two-phase ejectors; they first validated their model on an R11 refrigeration system. Based on the developed approach, the authors optimised the ejector geometry to achieve maximum values for either the entrainment ratio or the pressure ratio. Varga et al. (2009) investigated numerically (with a commercial Computational Fluid Dynamics package) the influence of selected geometry parameters, i.e., the area ratio between the motive nozzle and the mixer, the nozzle exit position, and the mixer length, on the steam ejector performance. The results indicated the existence of optimum values for all three examined parameters.

Elbel and Hrnjak (2008) experimentally studied a transcritical R744 system using a refrigerant ejector with different ejector dimensions such as the sizing of the motive nozzle and the size of the diffuser. According to the authors, small angles of divergence, $\alpha_{DIF} = 5$ °, yielded the best results for the static pressure recovery of the high-speed, two-phase flow entering the diffuser. Elbel (2011) presented more results on how the R744 ejector performance is affected by geometry variations, namely the diffuser divergence angle and the mixer length. The best ejector performance was again recorded for the lowest investigated value of the diffuser divergence angle, $\alpha_{DIF} = 5$ °; however, the author anticipated a potential for optimisation allowed by the trade-off between the kinetic energy losses caused by vortex formation and the losses caused by the frictional pressure drop. Additionally, the author obtained the highest values of ejector efficiency for the shortest variants of the mixer, where $L_{MIX}/D_{MIX} = 2.68$, which was believed to be caused by reduced frictional pressure drop and more favourable shock wave patterns in the mixing section. On the other hand, the selection of examined mixing section lengths did not allow determination of ejector performance reductions caused by incomplete mixing of the motive and the suction flows.

Nakagawa et al. (2011) experimentally analysed the effect of the mixer length on the R744 ejector system performance. The authors investigated three different variants of a rectangular-cross section mixer, finding that the pressure recovery profile along the mixing and the diffuser sections varied significantly for each mixing length. The optimum design was found for the middle option, $L_{MIX} = 15 \times 10^{-3}$ m, where the highest pressure recovery, suction flow rate, entrainment ratio, and overall system COP for all the conditions used in the experiments were obtained.

To investigate the possibility of using ejectors in domestic R744 heat pumps, a prototype ejector test facility was devised and manufactured at SINTEF Energi. In a previous investigation, Banasiak and Hafner (2011) showed that there was considerable potential for improvement of the COP, because the pressure ratio for the compressor could be reduced due to a significant pressure lift over the ejector. However, further investigation should be carried out to analyse the influence of the geometry parameters and the assembly combinations on the ejector performance.

Therefore, the main aim of the present paper was an experimental and numerical analysis of selected geometry aspects of flow passages on the R744 ejector performance. The influences of the mixer's diameter and length and the diffuser's divergence angle on the ejector's efficiency, suction pressure ratio and mass entrainment ratio were examined.

2. Test facility

All of the experiments were performed out at the R744 ejector test facility devised and assembled at SINTEF Energy Research. A transcritical R744 cycle consisted of the following processes (Fig. 1):

- 1–2: vapour phase compression in the piston-type compressor (a variable displacement OBRIST Engineering GmbH C99-5 unit with a frequency controller and a max. mass capacity of 0.11 kg s^{-1}),

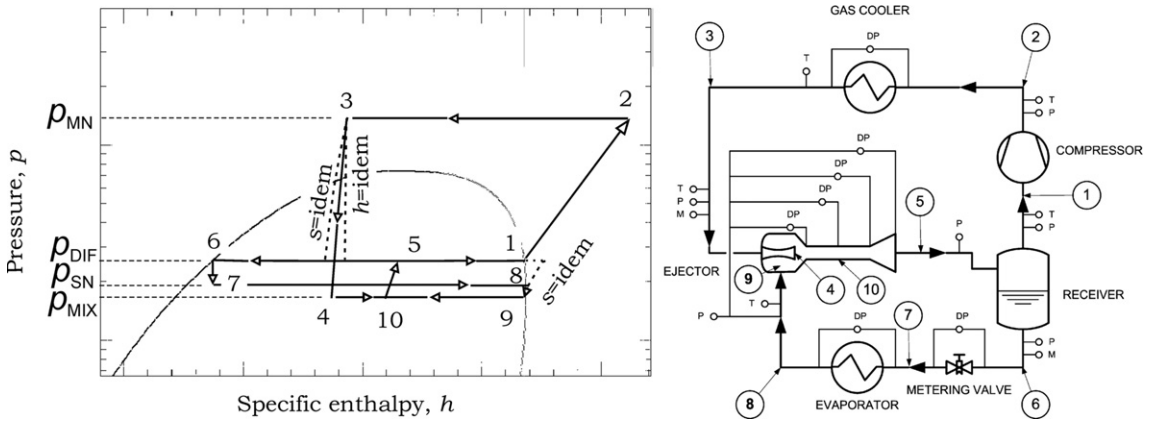

Fig. 1 – Schematic representation of an R744 transcritical cycle with a two-phase ejector for expansion work recovery (left) and schematics of the R744 ejector test facility (right). M – Coriolis-type mass flow meters, P – absolute pressure sensors, DP – differential pressure sensors, T – T-type thermocouples.

- 2–3: supercritical fluid cooling in the gas cooler (KAORI brazed plate heat exchanger, model no. K040C-20C),
- 3–4: expansion of the transcritical fluid in the motive nozzle (a prototype ejector assembly),
- 6–7: condensate expansion in the metering valve (HOKE 2300 bar stock valve with 8 ° stem point and 0.125" orifice),
- 7–8: flashing liquid evaporation in the evaporator (KAORI brazed plate heat exchanger, model no. K040C-20C),
- 8–9: vapour pressure drop in the suction nozzle (a prototype ejector assembly),
- 4–10 and 9–10: mixing of the primary and the secondary streams in the mixer (a prototype ejector assembly),
- 5–10: pressure growth in the diffuser (a prototype ejector assembly),
- 5–6 and 5–1: separation of the vapour–liquid mixture in the separator (a prototype design with multiple sight-glasses for liquid level monitoring).

The measurement system was based on temperature sensors (calibrated T-type thermocouples), absolute and differential pressure sensors (calibrated piezoelectric elements), and mass flow meters (calibrated Coriolis-type). The mean values of the measurement uncertainties, including both sensor accuracy and the time-averaged deviations from steady state, were as follows: $u(T) = \pm 0.3$ K, $u(P) = \pm 15 \times 10^3$ Pa, and $u(\dot{m}) = \pm 0.5 \times 10^{-3}$ kg s^{-1}.

The R744 two-phase ejector assembly consisted of a stainless steel nozzle section, brass mixing and diffuser sections, and a stainless steel ending section (see Fig. 2). The investigation into the influence of geometry was limited to different sizes of the mixer and the diffuser with a constant geometry of the motive nozzle.

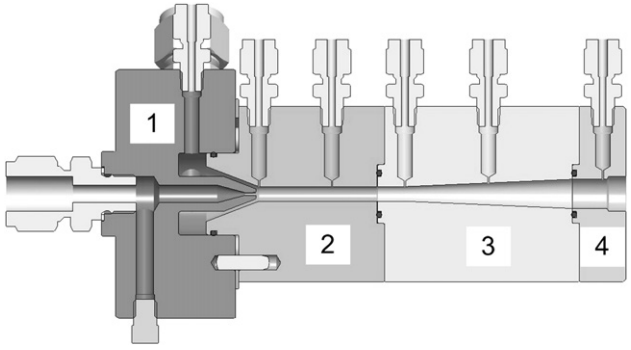

Fig. 2 – The ejector assembly. 1 – the nozzle section, 2 – the mixing section, 3 – the diffuser section, 4 – the ending section.

2.1. *Motive nozzle*

The experimental motive nozzle was manufactured as a converging-diverging conical channel bored in the head of the nozzle section body. The main construction parameters were as follows:

- Diameters: 6×10^{-3} m for the inlet cross section, 0.9×10^{-3} m for the throat cross section and 1.03×10^{-3} m for the outlet cross section.
- Angles of taper: 30 ° for the converging section and 2 ° for the diverging section.
- Wall surface roughness: approx. 1×10^{-6} m for both sections.

2.2. *Suction nozzle*

The suction nozzle geometry was determined by the walls of two surfaces: a conically chamfered head in the nozzle section and a conical inlet passage to the mixer. The cross-sectional area of the annularly formed suction nozzle could be adjusted by the distance rings, which varied the gap between the tip of the motive nozzle and the beginning of the mixing section, called the nozzle exit position. All of the tests reported in the paper were obtained for the nozzle exit position equal to 3.6×10^{-3} m.

2.3. *Mixer*

The mixer was manufactured as a straight tube with a conical inlet, which in combination with the nozzle section head created a suction nozzle. The convergence angle for the inlet

cone was set to 42 °, while the values of the internal diameter D_{MIX} for the produced pieces ranged from 2×10^{-3} m to 5×10^{-3} m, with a 1×10^{-3} m offset. The length of the passage had 3 options for each value of D_{MIX}: $L_{MIX} = 5 \times D_{MIX}$, $L_{MIX} = 10 \times D_{MIX}$, and $L_{MIX} = 20 \times D_{MIX}$, except for $D_{MIX} = 2 \times 10^{-3}$ m, which was limited only to two variants: $L_{MIX} = 10 \times D_{MIX}$ and $L_{MIX} = 20 \times D_{MIX}$.

2.4. *Diffuser*

The diffuser was formed as a conically diverging channel, where the total length of the passage was dependent on the inlet and the outlet diameters and the angle of divergence, α_{DIF}. The basic variants were manufactured with $\alpha_{DIF} = 5$ ° for each value of D_{MIX}, while additional variants with $\alpha_{DIF} = 7.5$ ° and $\alpha_{DIF} = 10$ ° were manufactured for the $D_{MIX} = 3 \times 10^{-3}$ m variant. The diffuser outlet diameters, $D_{DIF,out}$, were nominally manufactured to be 10×10^{-3} m; however, two additional versions with diameters of 6×10^{-3} m and 8×10^{-3} m were produced for the case where $D_{MIX} = 3 \times 10^{-3}$ m and $\alpha_{DIF} = 5$ °. Furthermore, the $D_{MIX} = 2 \times 10^{-3}$ m version was combined only with the smallest variant of the diffuser outlet diameter, $D_{DIF,out} = 6 \times 10^{-3}$ m.

3. Computational tools

The numerical simulations were performed by means of a code developed in house using the Visual Basic for Application environment. The computational tool included a 1D model of the R744 two-phase ejector and was validated for the critical mass flow rate and the pressure lift for typical heat pump operating conditions within the range of ±5% relative discrepancy, as described by Banasiak and Hafner (2011). However, because the analysis was focused on mixer and diffuser geometries only, and because of the requirement for an efficient computation process for the optimisation procedure, the time-consuming Delayed Equilibrium Model approach for a transcritical flow with delayed flashing over the motive nozzle was replaced by a simplified, but more time-efficient, Homogeneous Equilibrium Model. Therefore, the computational approach for both the motive and the suction nozzle used conservation equations for mass, momentum and energy in an incremental, 1D form. The governing equations were applied with the condition of adiabatic flow for a fluid in thermal and mechanical equilibrium, as well as the definition of isentropic efficiency for each passage, as described in Ouzzane and Aidoun (2003).

Refrigerant properties were evaluated using NIST subroutines contained in the REFPROP 8.0 database for all sections of the code.

Based on the results of the experimental tests, the simplified ejector model was validated and appropriately tuned to represent the behaviour of the two-phase ejector in an acceptably accurate manner. The validation procedure comprised two stages. First, the equivalent roughness of the mixing layer between the primary and the secondary streams and the mixing layer drag coefficient were adjusted, similarly as described in Banasiak and Hafner (2011). These adjustments were based on the results of 6 preliminary experimental tests performed with a single ejector geometry, with constant conditions at the motive/suction nozzle inlet and different levels of the mass entrainment ratio. The values of both parameters were adjusted for the mixer and the diffuser individually, based on the minimised sum of squared errors between the pressure profiles obtained during the initial 6 experiments and the pressure profiles generated by the simulation. In the second stage, the validation tests for various ejector geometries were carried out to verify the adjustments over a wider range of operating conditions and geometries. An additional 24 validation measurements were collected, where 3 different values for D_{MIX} were assessed, namely 3×10^{-3} m, 4×10^{-3} m and 5×10^{-3} m, each for the option of $L_{MIX} = 10 \times D_{MIX}$, $\alpha_{DIF} = 5$ °, and $D_{DIF,out} = 10 \times 10^{-3}$ m. The discrepancies between the simulation and the experiment results for the secondary stream pressure lift ranged between 0.5% and 9%.

It should be noted that the developed model as a 1D approach was incapable of explicit computational treatment of any shock-train phenomena, invoked by either overexpansion or underexpansion of the motive stream, occurring mostly in the mixing section. Therefore, all possible effects of the shock-train were included into the values of the two parameters being adjusted.

Moreover, all of the validation tests performed here comprised only the cases of 'subcritical' flow conditions for the secondary stream (typical for expansion work recovery ejectors), which was recognized by the existing possibility to increase the secondary stream mass flow rate by decreasing backpressure. This excluded the existence of oblique-shock-wave flow patterns occurring in diffuser in cases of chocked-suction-stream conditions. However, since the model does contain a simplified computational approach enabling to handle the phenomenon, Banasiak and Hafner (2011), the authors plan to perform additional laboratory experiments for the 'critical' conditions in the nearest future.

4. Ejector performance indicators

The key parameters for the thermodynamic and hydraulic evaluation of two-phase ejectors for expansion work recovery are the mass entrainment ratio, the suction pressure ratio and the ejector efficiency, Elbel and Hrnjak (2008).

The mass entrainment ratio defines the ratio between the suction mass flow rate of the ejector and the driving flow rate through the ejector motive nozzle. The ejector suction pressure ratio defines the elevated pressure of the refrigerant leaving the ejector in relation to the outlet evaporating pressure. The suction pressure ratio indicates the relative pressure increase by the ejector, which is recovered.

The ejector efficiency is defined as the ratio of the expansion work rate recovered by the ejector to the maximum possible expansion work rate, or the recovery potential. The amount of the expansion work rate recovered is defined as the product of the suction mass flow rate and the specific enthalpy difference identified by points 8 and 9_s. These points mark the beginning and the end of an imaginary, isentropic compression from the pressure of evaporation to the pressure of the diffuser outlet, which was taken away from the compressor's

duty and was replaced by the ejector operation. The maximum possible expansion work rate recovery potential is defined as the product of the motive mass flow rate and the specific enthalpy difference, identified by points 4_h and 4_s, which are at the ends of a theoretical, isenthalpic and isentropic expansion of the motive stream to the pressure of the diffuser outlet.

5. Ejector investigation

The experimental and numerical investigations were carried out for two sections of the R744 ejector – the mixer and diffuser – to investigate the influence of the geometry on the overall ejector performance.

5.1. *Results of experimental tests*

The analysis of the ejector geometries was performed for different levels of the motive stream inlet pressure, ranging from 80×10^5 Pa to 115×10^5 Pa. The adjustment of the discharge pressure was accomplished with a variable-speed compressor. The motive stream inlet temperature was kept constant at 303.7K ± 0.3 K by adjusting the cooling power of an auxiliary cooling loop, simulating the return line conditions for a space heating mode, Stene (2005). The suction–side parameters were kept constant for both pressure (35.5×10^5 Pa ± 0.07×10^5 Pa) and superheat (5K ± 0.5 K) by adjusting the heating power of an auxiliary water loop equipped with an electric heater and by regulating the metering valve opening.

Typical uncertainty values for the ejector parameters measured indirectly were as follows: ±0.009 for the mass entrainment ratio, ±0.003 for the suction pressure ratio, and ±0.03 for the ejector efficiency.

To investigate the influence of the diffuser divergence angle on the ejector performance, a series of 16 measurement points was taken. Three different divergence angles, $\alpha_{DIF} = 5\,^\circ$, $\alpha_{DIF} = 7.5\,^\circ$, and $\alpha_{DIF} = 10\,^\circ$, were analysed for the configuration with $D_{MIX} = 3 \times 10^{-3}$ m and $D_{DIF,out} = 10 \times 10^{-3}$ m. Furthermore, an additional diffuser piece characterised by $\alpha_{DIF} = 5\,^\circ$, $D_{MIX} = 3 \times 10^{-3}$ m, and $D_{DIF,out} = 8 \times 10^{-3}$ m was investigated. Fig. 3 presents the ejector efficiency vs. the motive nozzle inlet pressure and the suction pressure ratio vs. the mass entrainment ratio for different variants of the diffuser geometry. Although the presented profiles clearly indicate the advantage of lower values of the divergence angle, the differences in efficiency among the geometry options are rather moderate and are contained within the range of measurement uncertainty. Nevertheless, the obtained results are consistent with the conclusions drawn by Elbel and Hrnjak (2008) and Elbel (2011), where the most efficient performance of the R744 ejector was obtained for $\alpha_{DIF} = 5\,^\circ$.

To investigate the influence of the mixer length on ejector performance, a series of 12 measurement points was taken. Three mixer pieces with $L_{MIX} = 15 \times 10^{-3}$ m, $L_{MIX} = 30 \times 10^{-3}$ m, and $L_{MIX} = 60 \times 10^{-3}$ m were tested for the $D_{MIX} = 3 \times 10^{-3}$ m, $D_{DIF,out} = 10 \times 10^{-3}$ m, and $\alpha_{DIF} = 5\,^\circ$ case. Fig. 4 presents the ejector efficiency vs. motive nozzle inlet pressure and the suction pressure ratio vs. mass entrainment ratio for different variants of the mixer length. Although the difference in efficiency between the 15×10^{-3} m and 30×10^{-3} m cases was not significant, some trade-off potential was observed because the 15×10^{-3} m option offered higher efficiencies for a higher motive nozzle inlet pressure and lower efficiencies for the low-pressure region when compared to the 30×10^{-3} m case. The 60×10^{-3} m case evidently led to the lowest values of efficiency (the differences were reaching up to 10 percentage points for 112.5×10^5 Pa compared to the two other variants). Therefore, the mixer length analysis proved the considerable influence of friction forces on the mechanism of pressure recovery and indicated that the length optimisation procedure might be crucial for proper design. These findings were fairly consistent with the results reported by Nakagawa et al. (2011).

To investigate the influence of the mixer diameter on ejector performance, a series of 12 measurement points was taken. Mixing sections with $D_{MIX} = 2 \times 10^{-3}$ m, $D_{MIX} = 3 \times 10^{-3}$ m, and $D_{MIX} = 5 \times 10^{-3}$ m were examined, each for the case with $L_{MIX} = 10 \times D_{MIX}$, and $\alpha_{DIF} = 5\,^\circ$. Fig. 5 presents the ejector efficiency vs. motive nozzle inlet pressure and the suction pressure ratio vs. mass entrainment ratio for different

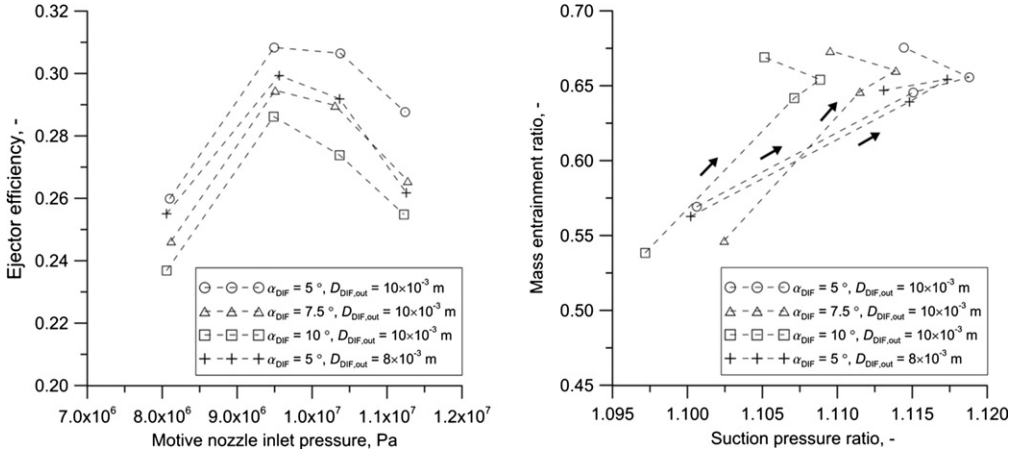

Fig. 3 – The experimental values of ejector efficiency (on the left) and the mass entrainment ratio and suction pressure ratio (on the right) for different diffuser geometries. Arrows in the right-hand-side graph indicate the direction of growing values of the motive nozzle inlet pressure.

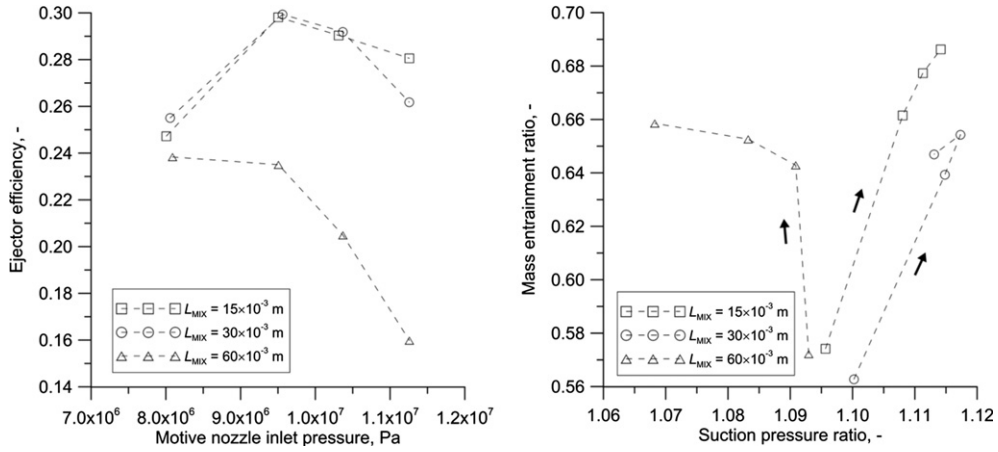

Fig. 4 – The experimental values of ejector efficiency (on the left) and the mass entrainment ratio and suction pressure ratio (on the right) for different mixer lengths. Arrows in the right-hand-side graph indicate the direction of growing values of the motive nozzle inlet pressure.

values of D_{MIX}. The highest values of ejector efficiency were recorded for the $D_{MIX} = 3 \times 10^{-3}$ m case over nearly the entire span of the motive nozzle inlet pressure. The difference in efficiency between the $D_{MIX} = 3 \times 10^{-3}$ m and $D_{MIX} = 5 \times 10^{-3}$ m cases was significant and ranged from approx. 18 percentage points for 80.5×10^5 Pa to approx. 13 percentage points for 112.5×10^5 Pa. Nevertheless, extrapolating the measured trends suggested that for certain conditions of the motive nozzle inlet pressure (far above 115×10^5 Pa), the $D_{MIX} = 5 \times 10^{-3}$ m case could perform more efficiently than the $D_{MIX} = 3 \times 10^{-3}$ m version. Additionally, a rapid drop in efficiency for the $D_{MIX} = 2 \times 10^{-3}$ m case over, approx., 81×10^5 Pa could be detected, probably as a consequence of the mass entrainment ratio being limited by the choking phenomenon occurring in the secondary flow. This suggests an additional optimisation procedure is possible at the design stage in terms of the duct diameter.

5.2. *Results of numerical simulations*

Based on the results of the experimental tests, the cases with 95×10^5 Pa and 103×10^5 Pa for the motive nozzle inlet pressure were selected for numerical investigation of the optimum ejector geometry. The mass entrainment ratio was held constant for each case separately and was equal to 0.68 for the 103×10^5 Pa case and 0.67 for the 95×10^5 Pa case. The other operational parameters as well as the geometry configuration were consistent with the settings for the experimental tests reported in Section 5.1.

The influence of the diffuser divergence angle on the ejector efficiency is presented in Fig. 6. The results showed the maximum efficiency may be reached at approx. 3 ° for the divergence angle for both cases, which was consistent with the data reported by Elbel (2011) as well as with the laboratory experiments described in Section 5.1. A rapid drop in

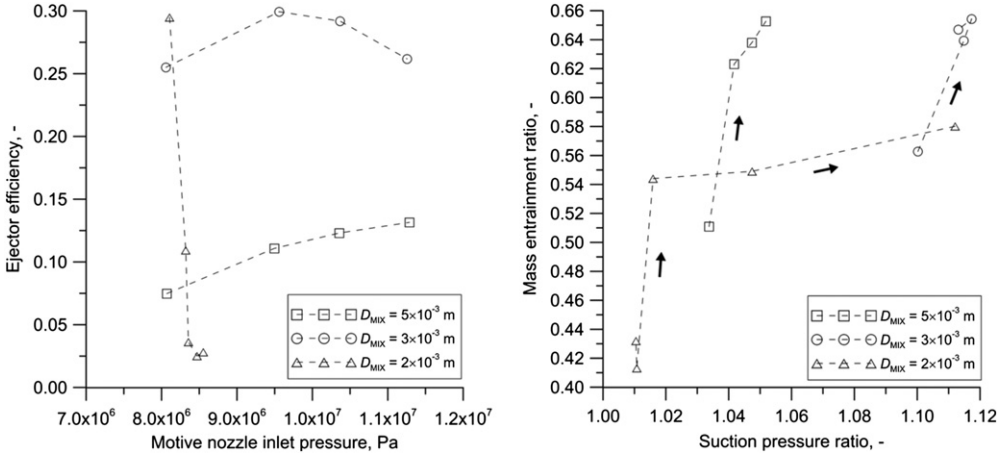

Fig. 5 – The experimental values of ejector efficiency (on the left) and the mass entrainment ratio and suction pressure ratio (on the right) for different mixer diameters. Arrows in the right-hand-side graph indicate the direction of growing values of the motive nozzle inlet pressure.

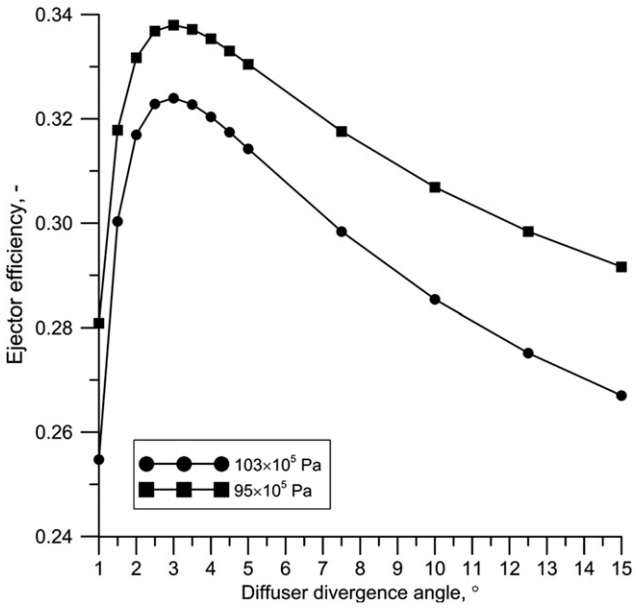

Fig. 6 – The simulated values of ejector efficiency as a function of the diffuser divergence angle; $D_{MIX} = 3 \times 10^{-3}$ m, $L_{MIX} = 30 \times 10^{-3}$ m, $D_{DIF,out} = 10 \times 10^{-3}$ m.

efficiency could be observed below approx. 2 °, due to the increased effects of wall friction, while only a gradual efficiency decrement above approx. 3.5 ° was observed, caused by incomplete momentum exchange in a shortened diffuser.

The influence of the mixer length on the ejector efficiency is shown in Fig. 7. The results confirmed the experimental results, where the maximum efficiency could be achieved for the lengths between 15×10^{-3} m and 30×10^{-3} m. Mixers shorter than approx. 10×10^{-3} m led to significantly decreased values of efficiency as a result of the limited area of momentum exchange, while mixers longer than approx. 40×10^{-3} m resulted in increased effects of wall friction.

The influence of the mixer diameter on the ejector efficiency is shown in Fig. 8. The simulations showed the maximum efficiency could be reached with $D_{MIX} = 3 \times 10^{-3}$ m for the 95×10^5 Pa case, and with $D_{MIX} = 3.5 \times 10^{-3}$ m for the 103×10^5 Pa case. These findings once again were consistent with the laboratory experiments performed previously. A rapid drop in efficiency could be observed below approx. 3×10^{-3} m, due to the secondary flow choking, while a gradual decrease above approx. 3.5×10^{-3} m was observed, the result of poorer momentum exchange.

6. System analysis

In addition to the ejector investigation, an experimental analysis for the overall system was performed, where the ejector-equipped heat pump was compared to a classic heat pump configuration with a traditional expansion valve. Based on the results of the previous test, the optimum ejector geometry was selected for the comparison tests (i.e., the mixer piece was 3×10^{-3} m in diameter and 30×10^{-3} m in length, combined with the diffuser having a 5 ° divergence angle and a 10×10^{-3} m outlet diameter). The motive nozzle inlet pressure was varied from 95×10^5 Pa to 110×10^5 Pa by adjusting the rotational speed of the compressor. The operating conditions for the gas cooler water loop were set to 303.2 K for the inlet and 343.2 K for the outlet for both expansion modes, simulating typical conditions for a space heating mode, Stene (2005). For each configuration, the inlet temperature of the low-temperature heat source (maintained by an auxiliary water loop) was 293.2 K, while 5 K of superheat

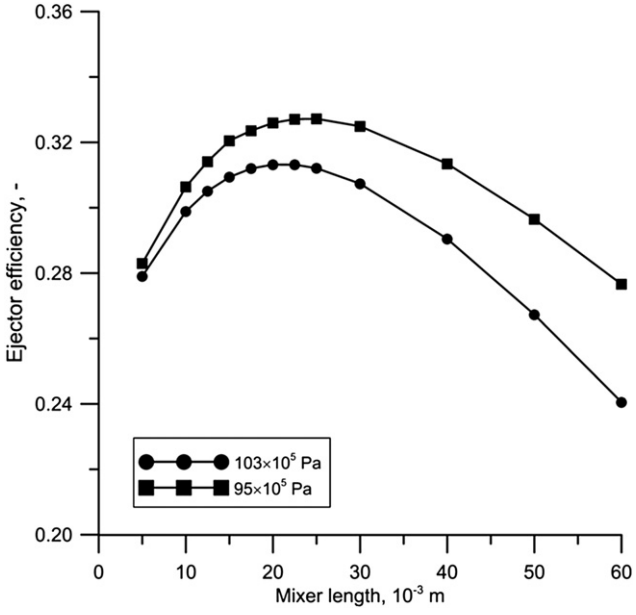

Fig. 7 – The simulated values of ejector efficiency as a function of the mixer length; $D_{MIX} = 3 \times 10^{-3}$ m, $D_{DIF,out} = 10 \times 10^{-3}$ m, $\alpha_{DIF} = 5$ °.

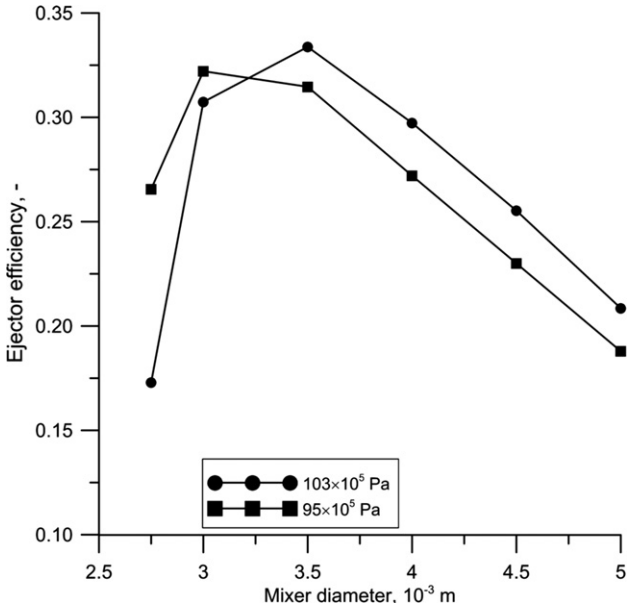

Fig. 8 – The simulated values of ejector efficiency as a function of the mixer diameter; $L_{MIX} = 10 \times D_{MIX}$, $D_{DIF,out} = 10 \times 10^{-3}$ m, $\alpha_{DIF} = 5$ °.

Table 1 – Energy performance of the examined heat pump system, operated either with a classic expansion valve or the ejector.

Heating capacity, kW Average uncertainty: ±0.13 kW	Ejector efficiency (ejector system) Average uncertainty: ±0.03	COP (ejector system) Average uncertainty: ±0.11	COP (expansion valve system) Average uncertainty: ±0.11	Relative COP difference
5	0.259	3.70	3.46	6.63%
6	0.290	3.63	3.38	6.91%
7	0.306	3.57	3.31	7.23%
8	0.310	3.51	3.25	7.57%
9	0.307	3.45	3.18	7.89%
10	0.297	3.38	3.10	8.14%
11	0.282	3.29	3.02	8.27%
12	0.263	3.18	2.92	8.26%
13	0.238	3.05	2.80	8.02%

was maintained at the evaporator outlet for floating levels of evaporation pressure. This made the performance of both expansion modes comparable. However, it should be noted that the system was not optimised by the COP maximisation for either of the two analysed options. The results of the energy analysis for the heat pump COP are presented in Table 1.

The maximum COP increase (the last column) was registered for the upper region of heating capacity, while the ejector efficiency (the second column) reached its maximum for the intermediate load. However, since the ejector efficiency profile is rather plane and represents high values along the whole analysed span, the authors find it, together with constant temperature at the motive nozzle inlet, the main reason for which the achieved COP improvement may be considered relatively constant.

Nevertheless, to maximise the potential COP gains, it is necessary to construct the analysed system with the ejector having the geometry optimised strictly for a given application. Therefore, a global optimisation procedure aimed at the maximisation of the overall system COP would be recommended.

7. Conclusions

A transcritical R744 system with an ejector for expansion work recovery showed considerable potential for COP improvement. The experimental investigation performed at the SINTEF laboratory revealed that the COP of the ejector-equipped system could be up to 8 percentage points higher than for the system with a classic expansion valve at the specific test conditions (for non-optimised systems).

Based on the experimental tests, the 5 ° divergence angle proved to yield the highest values of the ejector efficiency among all geometry options examined. In addition, it was observed that the larger the diameter at the outlet of the diffuser, the better the performance.

During the experimental tests, the best results were achieved for the mixer length equal to 30×10^{-3} m. Shorter options produced relatively similar results; however, the momentum exchange potential seemed to be utilised only partially. For longer sections, the pressure drop caused by friction forces occurred along the duct and significantly reduced the pressure lift generated by the ejector.

The impact of the mixing section diameter on ejector operation was experimentally tested as well. It was demonstrated that the best performance was achieved for the 3×10^{-3} m diameter. For smaller diameters, the ejector was not able to entrain the appropriate amount of superheated vapour from the evaporator at higher pressure values. The phenomenon was most likely caused by throttling of the secondary flow in the mixer and a consecutive oblique-shock-wave flow pattern. For larger diameters, the ejector was unable to achieve high values of either pressure lift or efficiency because of the poorer momentum exchange, possibly as a result of intensified recirculation.

The results of the computational investigation showed that the optimum diffuser angle was approx. 3 °. The optimum length of the mixing section depended on the inlet pressure to the motive nozzle and was between 20 mm and 25 mm. The calculations for the optimum diameter revealed that for lower pressures, smaller diameters were advisable, while for higher pressures, the situation was reversed.

To maximise the potential COP gain resulting from the use of an ejector, the COP of the overall system should be optimised, which will constitute the next step in forthcoming research.

Acknowledgements

The research was supported by a grant from Norway through the Norwegian Financial Mechanism under contract no. PNRF - 150 - A I – 1/07.

REFERENCES

Banasiak, K., Hafner, A., 2011. 1D computational model of a two-phase R744 ejector for expansion work recovery. Int. J. Therm. Sci. 50, 2235–2247.

Cizungu, K., Groll, M., Ling, Z.G., 2005. Modelling and optimization of two-phase ejectors for cooling systems. Appl. Therm. Eng. 25, 1979–1994.

Elbel, S., Hrnjak, P., 2008. Experimental validation of a prototype ejector designed to reduce throttling losses encountered in transcritical R744 system operation. Int. J. Refrig. 31, 411–422.

Elbel, S., 2011. Historical and present developments of ejector refrigeration systems with emphasis on transcritical carbon dioxide air-conditioning applications. Int. J. Refrig. 34, 1545–1561.

Nakagawa, M., Marasigan, A.R., Matsukawa, T., Kurashina, A., 2011. Experimental investigation on the effect of mixing length on the performance of two-phase ejector for CO_2 refrigeration cycle with and without heat exchanger. Int. J. Refrig. 34, 1604–1613.

Ouzzane, M., Aidoun, Z., 2003. Model development and numerical procedure for detailed ejector analysis and design. Appl. Therm. Eng. 23, 2337–2351.

Stene, J., 2005. Residential CO_2 heat pump system for combined space heating and hot water heating. Int. J. Refrig. 28, 1259–1265.

Varga, S., Oliveira, A., Diaconu, B., 2009. Influence of geometrical factors on steam ejector performance – a numerical assessment. Int. J. Refrig. 32, 1694–1701.